



Non-aqueous reverse micelles created with a cationic surfactant: Encapsulating ethylene glycol in BHDC/non-polar solvent blends



Dr. Federico M. Agazzi, Dr. R. Dario Falcone, Prof. Dr. Juana J. Silber, Prof. Dr. N. Mariano Correa*

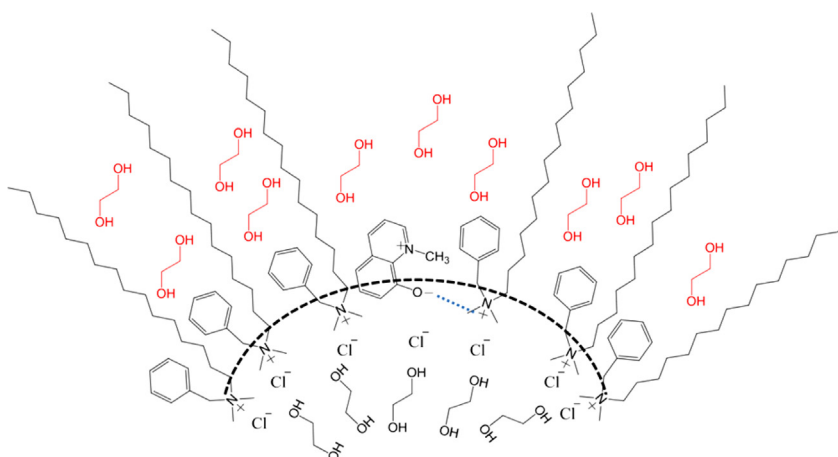
Departamento de Química, Universidad Nacional de Río Cuarto, Agencia Postal # 3, C.P X5804BYA Río Cuarto, Argentina

HIGHLIGHTS

- Non-aqueous reverse micelles are created without the addition of cosurfactant.
- This is the first report where stable EG/BHDC reverse micelles are formed and characterized.
- EG solubilization capacity depends on the external phase composition, and decreases as the *n*-heptane content increases.
- The micellar size increases when *n*-heptane content increases.
- *n*-heptane favors the droplet-droplet attractions.

GRAPHICAL ABSTRACT

EG and BHDC can form stable non-aqueous reverse micelles in benzene:*n*-heptane solvent blends without the needing of co-surfactant.



ARTICLE INFO

Article history:

Received 4 August 2016
Received in revised form
15 September 2016
Accepted 16 September 2016
Available online 17 September 2016

Keywords:

Non-aqueous reverse micelles
BHDC
QB
DLS

ABSTRACT

We present results on a new system that forms non-aqueous reverse micelles (RMs) created with a cationic surfactant, benzyl-*n*-hexadecyldimethylammonium chloride (BHDC), encapsulating ethylene glycol (EG), in different nonpolar solvents blends of *n*-heptane:benzene. It is shown that a cationic surfactant forms RMs using EG as polar solvent without the addition of a co-surfactant. In particular, we analyzed the EG solubilization capacity, the droplet size values and the interface composition of EG/BHDC/*n*-heptane:benzene RMs, using dynamic light scattering (DLS) and the solvatochromic behavior of 1-methyl-8-oxyquinolinium betaine (QB) as molecular dye.

The EG solubilization capacity depends on the external phase composition decreasing when the *n*-heptane content increases. Using DLS technique, we demonstrate the formation of RMs, and observe that for the same [EG]/[BHDC] ratio, the micellar size increases when *n*-heptane content increases.

Using QB it was found that EG penetrates into the micellar interface changing dramatically the composition and the droplet-droplet interaction, in comparison when water is encapsulated.

© 2016 Elsevier B.V. All rights reserved.

1. Introduction

When a surfactant is dispersed in a non-polar solvent, under specific conditions they may self-assemble to form reverse micelles

* Corresponding author.

E-mail address: mcorrea@exa.unrc.edu.ar (N.M. Correa).

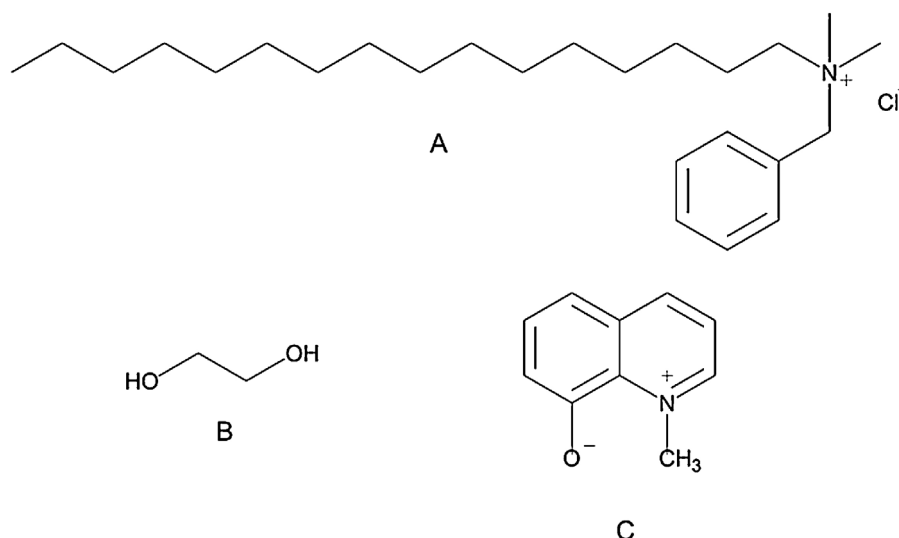


Fig. 1. Molecular structure of (A) BHDC, (B) EG, and (C) QB.

(RMs) aggregates. The interesting fact of RMs is that they can dissolve a polar solvent in their polar core. [1–3] Due to the large diversity of nano-environments that these systems provide, such as the micellar core and the interface, RMs have found a wide range of applications in different areas [4–6].

The nature of the encapsulated solvents make it possible to discriminate between aqueous [7] and non-aqueous RMs [8]. To characterize RMs, it is useful to introduce a quantitative parameter, W_s , which is frequently associated with the micellar size, and defined in terms of the ratio between the molar concentration of the polar solvent and surfactant namely $W_s = [\text{Polar Solvent}]/[\text{Surfactant}]$. When the polar solvent is water, the molar ratio is defined as W_0 [7].

Depending on the head-group charge of the surfactant molecules they may be nonionic, anionic, cationic and zwitterionic. One of the most widely used surfactant is the anionic AOT (sodium 1,4-bis-2-ethylhexyl sulfosuccinate) [2,3,9–12] On the other hand, the analyses of cationic RMs have been mostly performed in systems composed by quaternary aliphatic ammonium salts, such as cetyltrimethylammonium bromide (CTAB) [13–15]. It must be highlighted that those systems require the use of alcohols in order to form stable RMs. In this paper we will focus our attention on a less employed cationic surfactant: benzylhexadecyldimethyl-

lammonium chloride, or BHDC (Fig. 1A) which is an interesting cationic surfactant that does not need a co-surfactant to form stable RMs [7,16,17]. Until recent years, the BHDC surfactant had been employed only to produce RMs dispersed in pure aromatic solvents, such as benzene, and mostly using water or ionic liquid as the polar solvent to be encapsulated [18–21].

Recent studies performed using experimental techniques [7,17,22] and computer simulation [17], have shown that water/BHDC RMs can also be formed in mixtures of *n*-heptane:benzene. At a given value of W_0 , we observed that the droplet sizes increase as the proportion of *n*-heptane in the solution increases. On the other hand, the local micropolarity of the environment and the magnitude of the water-surfactant interaction were found to change dramatically with the composition of the nonpolar phase. The results were rationalized by taking into account the magnitude of the solvent penetration into the interface and its influence over both the droplet-droplet interaction and the water structure inside the RMs.

All the studies mentioned above using BHDC as surfactant, had used water, as the polar constituent encapsulated in the RMs. However, considering the application of RMs as solubilization medium or as nanoreactors, many organic reactants are not easily solubilized in water and, moreover, dielectric constants at the interface of aqueous organized media are lower than in water, and are close to those found in salt solutions or in methanol [8]. These considerations led us to the use of non-aqueous solvents, such as propylene glycol (PG), ethylene glycol (EG, Fig. 1B), and formamide (FA), that enhance solubility and reactivity in microheterogeneous media, such as RMs [8].

In this context, due to the limited investigations on non-aqueous cationic RMs, can be helpful to investigate RMs systems using BHDC as cationic surfactant, and EG as a polar solvent highly immiscible in non-aqueous solvent (such as benzene and *n*-heptane). We chose EG as the polar solvent because recently it has received increasing interest in the non-aqueous category of solvents and, has been applied in different application from photophysical studies to nanoreactor and enzymatic reaction [23–31]. Moreover, this solvent has been studied by Durantini et al. [10] using AOT RMs. In addition, given the “modulatory effect” of the external phase on the properties of water/BHDC RMs previously demonstrated [7,16,17], we will use solvent mixtures as external non-polar phase to investigate its effect on the new non-aqueous BHDC RMs presented herein.

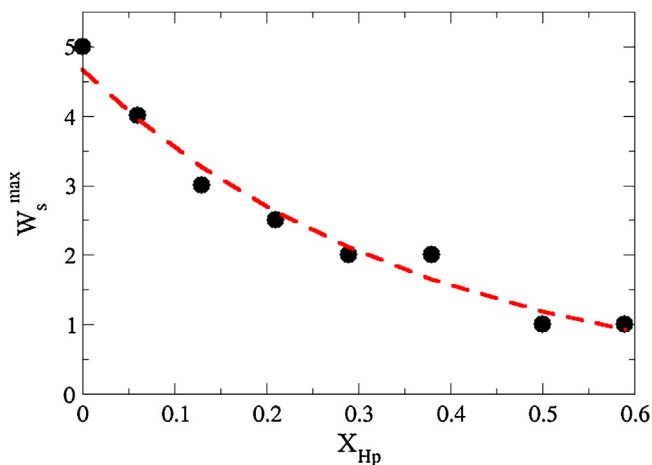


Fig. 2. Ethylene glycol (EG) maximum solubilization capacity, W_s^{max} , for EG/BHDC/*n*-heptane:benzene RMs. [BHDC]=0.10 M. T=25 °C.

Thus, we study the new RMs media formed with EG/BHDC/*n*-heptane:benzene focusing the attention on the following: (i) the possibility of forming stable ternary systems comprised of EG/BHDC/*n*-heptane:benzene; (ii) the determination of the EG maximum solubilization capacity in the ternary systems; (iii) the formation or absence of an organized system consisting of RMs, and the functionality between micellar size, EG content (expressed by the molar ratio WS) and external phase composition (expressed by molar fraction of *n*-heptane X_{Hp}) using dynamics light scattering (DLS) and, (iv) the determination of the interfacial composition and interactions using an absorption molecular probe, the 1-methyl-8-oxyquinolinium betaine, QB (Fig. 1B). In all cases, we established comparisons between the behaviors of EG/BHDC RMs and water/BHDC RMs previously studied [7,16,17]. Furthermore comparison between the properties of EG/BHDC cationic RMs and EG/AOT anionic RMs was also carried out.

We show that using DLS and spectroscopy techniques (using molecular probes like QB) is very helpful to guarantee that RMs are formed instead of structureless microemulsion. As it was previously described in reference [8], it is known that all RMs are w/o microemulsion but, not all w/o microemulsions are RMs. It is necessary that the RMs solutions have the following characteristics, that differ from microemulsion with no structure (structureless microemulsion): (a) it contains individual particles that move freely in the non-polar solvent; (b) there is a clear interface that separates polar from non-polar components; (c) three different phases are clearly identified and includes the non-polar phase, the polar phase and the interface; (d) the size of the particle depends on the amount and structure of the polar solvent used.

2. Experimental methodology

2.1. Materials

Benzene and *n*-heptane (Merck, HPLC grade) were used as received. The polar solvent ethylene glycol (EG) from Aldrich (more than 99% of purity) was used without further purification. Benzyl-*n*-hexadecyldimethylammonium chloride (BHDC) (Sigma >99% purity) was purified as described elsewhere [21]. 1-Methyl-8-oxyquinolinium betaine (QB) was synthesized using the description showed in the literature [32].

2.2. Procedure

The *n*-heptane:benzene solutions were prepared by weight, at any of the *n*-heptane bulk molar fraction, X_{Hp} , investigated. The BHDC stock solutions in the solvent mixtures were prepared by weight followed by a solvent dilution. EG was added to the system using a microsyringe. The amount of EG dissolved in the RMs media is defined as $W_s = [EG]/[BHDC]$, which is the molar ratio between EG and BHDC. $W_s = 0$ represents the RMs without the addition of the glycol.

A stock solution of 0.01 M in methanol was prepared for QB. To prepare the solutions with the QB concentration used in the RMs media, 2×10^{-4} M, the proper amount of the stock solution was put into a volumetric flask. The methanol solvent was evaporated under a flow of dry N_2 . After that, the BHDC RMs solution was added to the solid to obtain the stock surfactant concentration of 0.20 M, which were used to prepare all the other solutions with different surfactant concentrations.

2.3. General details

2.3.1. Absorption spectroscopy

All the experiments were carried out at 25.0 °C. UV–vis spectra were obtained using a spectrophotometer Shimadzu 2401 with a

Table 1

Maximum solubilization capacity for EG (W_s^{\max}) and water (W_0^{\max}), in BHDC/*n*-heptane:benzene RMs^a.

X_{Hp}	W_s^{\max}	W_0^{\max} ^b
0.00	5.0	25.0
0.06	4.0	20.0
0.13	3.0	18.0
0.21	2.5	6.0
0.29	2.0	5.0
0.38	2.0	2.0
0.59	1.0	1.0

^a [BHDC] = 0.10 M.

^b W_0^{\max} values obtained from reference [7].

thermostated sample holder. A cell with a path length of 1 cm was used in every experiment.

2.3.2. Dynamics light scattering

The RMs apparent hydrodynamic diameters were determined using dynamic light scattering. (DLS, Malvern 4700 with goniometer). The laser used is an argon-ion operating at 488 nm. The RMs solutions were filtered prior to the experiments using a Sigma PTFE Acrodisc membrane of 0.2 μ m. The parameters needed for the solvent mixtures, viscosities and refractive indexes, were obtained from literature and the methodology employed were described elsewhere [7,33].

To obtain statistic reliable results, 30 independent size measurements were taken for each of the samples. The scattering angle used was ninety degrees. CONTIN was used as the algorithm to obtain the apparent hydrodynamic diameter values. The polydispersity found for the different solutions investigated is always less than 5%.

3. Results and discussion

3.1. Ethylenglycol maximum solubilization capacity

We will first focus in the EG maximum solubilization capacity, define as $W_{s\max} = [EG]_{\max}/[BHDC]$, of BHDC in different *n*-heptane:benzene mixtures. It is noteworthy that EG is not significantly soluble in benzene, heptane and its mixtures [8]. Fig. 2 shows the $W_{s\max}$ values as a function of the molar fraction of *n*-heptane, X_{Hp} , for EG/BHDC/*n*-heptane:benzene systems. In all systems, we observed a transparent and stable single phase for $W_s \leq W_{s\max}$ values. Above this threshold, the media becomes cloudy because the phase transition occurs. It is worth to note that, for the first time, it was possible to solubilize the polar solvent EG in the cationic BHDC RMs, using different external non-polar phases. It is observed that a maximum $W_{s\max} \approx 5$ value is reached in pure benzene, i.e., $X_{Hp} = 0.00$, and the $W_{s\max}$ values decrease upon the addition of *n*-heptane.

At this point it is instructive to compare with previous results obtained using water as the dispersed solvent. In previous work [7], we investigated the water solubility capacity, define as $W_{0\max} = [Water]_{\max}/[BHDC]$, for water/BHDC/*n*-heptane:benzene systems, and observed a similar trends between $W_{0\max}$ and the *n*-heptane content. Thus, for BHDC/*n*-heptane:benzene systems, the polar solvents solubility capacity decreases when increases the aliphatic solvent content in the external non-polar phase. However, as it is observed in Table 1, for each external phase composition, $W_{s\max} \ll W_{0\max}$, which means that the EG solubility capacity is smaller than the water solubility capacity. For example, (i) at $X_{Hp} = 0.00$, the $W_{0\max} = 25$, and $W_{s\max} = 5$ which is about five times smaller, (ii) at $X_{Hp} = 0.21$, the $W_{0\max} = 6$, and $W_{s\max} = 2$ which is about three times smaller. In the next section, we will propose a possible interpretation of these differences.

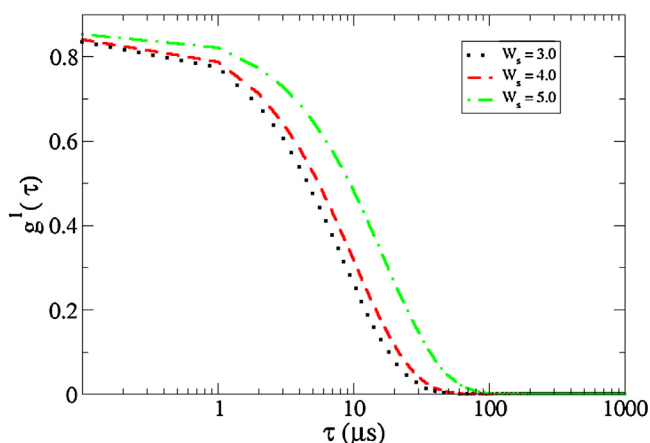


Fig. 3. Typical DLS measured correlograms of the scattered intensity from EG/BHDC/benzene RMs at different W_s . [BHDC] = 0.10 M. $T = 25^\circ\text{C}$.

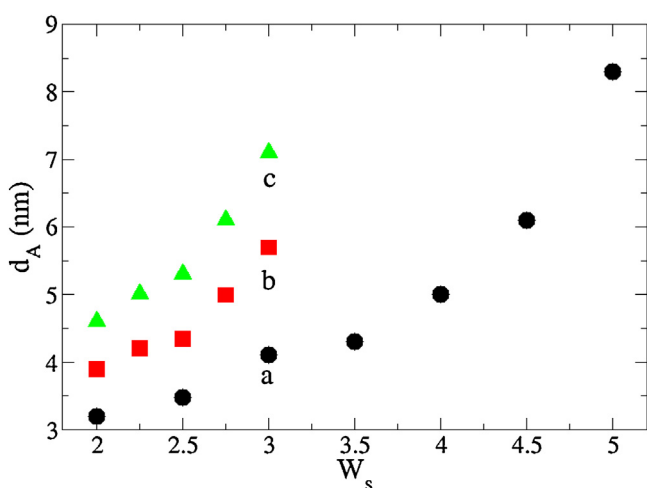


Fig. 4. EG/BHDC/*n*-heptane:benzene droplets apparent diameters, d_A , as a function of W_s for (a) $X_{\text{HP}} = 0.00$, (b) $X_{\text{HP}} = 0.13$, and (c) $X_{\text{HP}} = 0.21$. [BHDC] = 0.10 M. $T = 25^\circ\text{C}$.

3.2. Dynamic light scattering

In the previous section, we showed that EG can be dispersed by BHDC surfactant in *n*-heptane:benzene mixtures but, is EG effectively sequestered by BHDC forming RMs media in every solvent mixtures investigated?. Dynamics light scattering, DLS, is an interesting technique to evaluate this issue [7,34,35]. If EG is encapsulated to give RMs then, the droplets size values must also increase with W_s . If this happens, it is because of EG molecules are not solubilized in the external non-polar phase [7]. Fig. 3 shows typical correlograms of the DLS experiments for BHDC RMs in benzene, at $W_s = 3.0$, $W_s = 4.0$ and $W_s = 5.0$. Similar results were obtained for the other RMs in the different solvents blends (results not shown). Fig. 4 shows the apparent hydrodynamic diameter values, d_A , as a function of W_s , for EG/BHDC/*n*-heptane:benzene systems at different solvent blends with $X_{\text{HP}} = 0.00$, 0.13 and 0.21, and [BHDC] = 0.10 M. In all the systems monitored, it can be observed that when the W_s values increase, the d_A values also increase. This tendency shows that EG molecules are effectively sequestered by BHDC surfactant molecules, yielding non-aqueous cationic RMs, in every solvent mixture investigated. Moreover, the droplet size values of the different RMs were obtained at different days and no variation was observed. This makes us confident that the RMs are thermodynamically stable. Riter et al. [36] explored EG/AOT/isooctane anionic

Table 2

Droplets apparent diameters (d_A) for BHDC/benzene:*n*-heptane RMs encapsulating water or EG^a.

X_{HP}	W	Water ^b	d_A (nm) EG
0.00	5.0	5.0	8.5
0.13	3.0	4.0	5.5

^a [BHDC] = 0.10 M.

^b d_A values for water/BHDC RMs were obtained from reference [7].

RMs through DLS, and they obtained a similar tendency with W_s and similar droplet micellar sizes.

Herein, some features deserve some comments. The droplet sizes for BHDC RMs in benzene ($X_{\text{HP}} = 0.00$) are significantly smaller than the droplet sizes in the solvent mixtures. Thus, at W_s fixed, when the *n*-heptane content increases, the size of aggregates also increases. For example, at $W_s = 3$, the droplet size is (i) 3.0 nm in $X_{\text{HP}} = 0.00$, (ii) 5.5 nm in $X_{\text{HP}} = 0.13$, and (iii) 7.0 nm $X_{\text{HP}} = 0.21$. In previous work [7], we obtained a similar trend for water/BHDC RMs in *n*-heptane:benzene mixture. The explanation that we proposed to explain those results was that *n*-heptane in the external non-polar phase, increases the inter-droplets attractive interactions, with the consequent increment in the droplet size [7]. As the benzene concentration increases, the inter-droplet attractive interactions are “switched off” and decreases in magnitude.

Moreover, to obtain a molecular view of the process, in a more recent work, we studied the influence of the external phase on the inter-micellar interactions, using molecular dynamics simulation in water/BHDC/*n*-heptane:benzene [17]. We determined the free energy profile by the coalescence process between two RMs of similar size, in pure benzene and, in a *n*-heptane:benzene mixture. The results showed that the free energy barrier is lower for the RMs made in mixed solvents. Therefore, we were led to conclude that the difference in the overall shape and size of both solvent molecules would lead to a less efficient packing, that is, a more straightforward release, of the *n*-heptane molecules in the inter-micellar domain, leading to an overall reduction in the local free energy barriers controlling the association process [17]. Then, the results reported in Fig. 4, show that the same analysis can be extrapolated to the EG/BHDC RMs: as the *n*-heptane content increases, the inter-droplet attractive interaction also increases (due to the more straightforward release of the *n*-heptane molecules from the interface), with the consequent increment in the size of micellar aggregates. This seems to be a common trend when protic solvents like water and EG are confined to a nanometer scale, independently on the surfactant used [7].

On the other hand, can be instructive to compare the droplets size for water/BHDC and EG/BHDC RMs at similar polar solvent content. Table 2 shows the d_A values, for water/BHDC/*n*-heptane:benzene [7] and EG/BHDC/*n*-heptane:benzene RMs, for two molar fractions of *n*-heptane X_{HP} , at [BHDC] = 0.10 M. It can be observed that the d_A values are larger for EG/BHDC RMs than for water/BHDC RMs, at the same W_s and X_{HP} values. This result suggests that the attractive interactions between RMs are favored in the presence of EG, which could generate larger aggregates. This is not surprising since it is known that EG penetrates deeply the AOT RMs interface making it less rigid and prompt to favor the droplet-droplet interactions [8].

The fact that the droplet-droplet interactions are favored when EG is encapsulated, would explain the significant decreases in the EG solubilization capacity obtained for EG/BHDC RMs, compared to water/BHDC RMs (Table 1). In EG/BHDC/*n*-heptane:benzene RMs, some of EG molecules would penetrate into the micellar interface and could affect the packing parameter surfactant molecules, defined as $P = v/al$ where v and l are the volume and the length of the surfactant tails and, a is the surface area of the surfac-

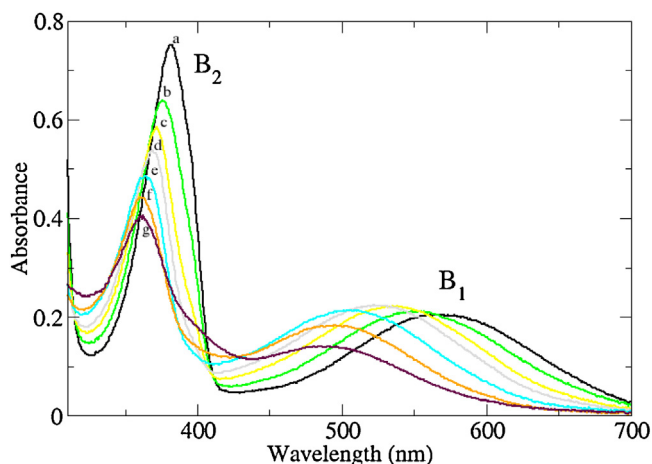


Fig. 5. QB absorption spectra in EG/BHDC/*n*-heptane:benzene RMs at $X_{Hp} = 0.00$, $W_s = 2.5$ and different BHDC concentration: (a) 0.00 M, (b) 4.92×10^{-4} M, (c) 1.95×10^{-3} M, (d) 7.81×10^{-3} M, (e) 2.69×10^{-2} M, (f) 0.10 M and (g) 0.20 M. $[QB] = 2 \times 10^{-4}$ M.

Table 3

Critical Micellar Concentration (cmc) for EG/BHDC/*n*-heptane:benzene RMs at $W_s = 0.0^a$ and 2.5, and at different X_{Hp} , obtained by QB solvatochromism. $[QB] = 2.0 \times 10^{-4}$ M.

X_{Hp}	cmc (M)	
	$W_s = 0.0^a$	$W_s = 2.5$
0.00	$(1.0 \pm 0.2) \times 10^{-2}$	$(7.6 \pm 0.2) \times 10^{-3}$
0.13	$(6.0 \pm 0.2) \times 10^{-3}$	$(2.2 \pm 0.2) \times 10^{-3}$
0.21	$(4.0 \pm 0.2) \times 10^{-3}$	$(3.3 \pm 0.2) \times 10^{-4}$

^a Values obtained from reference [7].

tant headgroups [7]. Thus, the EG penetration could increase the tails effective length by disfavoring of the folding of the surfactant tails with the consequent increase in the l value. This produces a decrease in P and increases the interfacial fluidity. Thus, the micellar interface is more fluid in EG/BHDC compared to water/BHDC RMs, increasing the inter-droplets attractive interactions, and diminishing the stability and solubilization capacity of EG/BHDC RMs. Durantini et al. [10] investigated EG/AOT/*n*-heptane RMs using FT-IR technique monitoring the AOT carbonyl and sulfonyl vibrational modes. They demonstrated that EG molecules penetrate into the oil side of the interface, and interact through hydrogen bonding with AOT C=O group. In EG/BHDC RMs, there is not possibility of a specific interaction between EG and BHDC, such as the hydrogen bonding observed in EG/AOT RMs, therefore, EG molecules located into the BHDC RMs interface would have more mobility, and its average localization could be somewhat different to the one observed in EG/AOT RMs. In order to obtain additional evidences about the average localization and interaction of EG molecules with the cationic interface, we used an absorption molecular probe, QB. The main results obtained with QB as molecular probe are shown in the next section.

3.3. Studies using QB as molecular probe

QB molecule (Fig. 1C) presents two electronic absorption bands, B_1 and B_2 , which sense different effects as we have previously demonstrated [9,20]. It is known that the solvatochromism of the B_1 band, the one located in the visible region, is mainly due to the polarity/polarizability ability of the solvent. However, this band also correlates with the hydrogen bond donor ability of the medium. With increasing the polarity or the hydrogen bonds donor ability of the solvent, the ground state becomes more stable, which

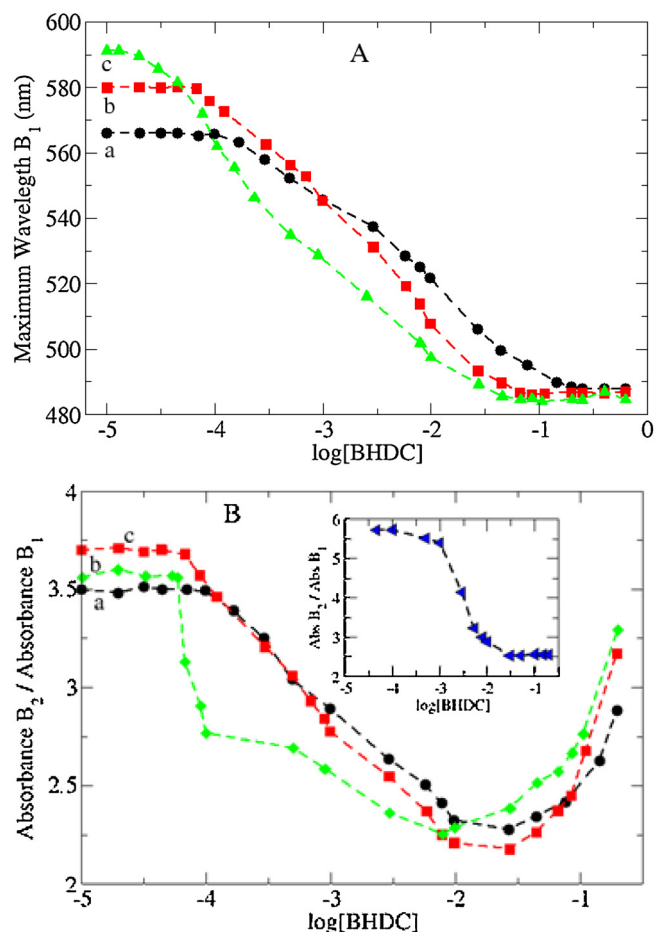


Fig. 6. (A) Maximum wavelength B_1 values and (B) Absorbance B_2 /Absorbance B_1 ratio values, as a function of $\log[BHDC]$ for EG/BHDC/*n*-heptane:benzene RMs, at $W_s = 2.5$, and X_{Hp} values of (a) 0.00, (b) 0.13 and (c) 0.21. The inset in panel B, extracted from reference 7, show the Absorbance B_2 /Absorbance B_1 ratio values, as a function of $\log[BHDC]$ for water/BHDC/*n*-heptane:benzene RMs, at $W_0 = 5:0$, and $X_{Hp} = 0.21$. $[QB] = 2 \times 10^{-4}$ M.

leads to an increase in the transition energy, that is, the band shows negative solvatochromism [9].

The B_2 band, the one located in the UV region, also shifts hypsochromically with the polarity of the solvent, although in lesser magnitude than the visible band [9]. Moreover, it was shown that the B_2 band wavelength is also sensitive to the hydrogen bond donor capability of the solvent. The absorbance ratio of both bands ($Abs B_2 / Abs B_1$) is sensitive to the hydrogen bond ability of the solvent. $Abs B_2 / Abs B_1$ value decreases as the solvent hydrogen bond capability increases [9]. In addition, we demonstrated in previous works that the $Abs B_2 / Abs B_1$ ratio is also sensitive to electrostatic interactions which make even stronger the versatility of QB as molecular probe [7].

It is important to note that despite that QB is soluble in benzene and can undergoes a partition process between two different pseudophases, the RMs and the organic solvent, we have previously shown in water/BHDC/benzene [21] and 1-butyl-3-methylimidazolium tetrafluoroborate or 1-butyl-3-methylimidazolium bis-(trifluoromethylsulfonyl) imide/BHDC/benzene [20] at any polar solvent content, that the molecular probe resides mainly at the RMs interface because of a strong interaction between the cationic polar head of the surfactant and the QB aromatic ring. Thus, QB can monitor the changes at the BHDC RMs interfaces, probably at the same level as the surfactant headgroup [7,16].

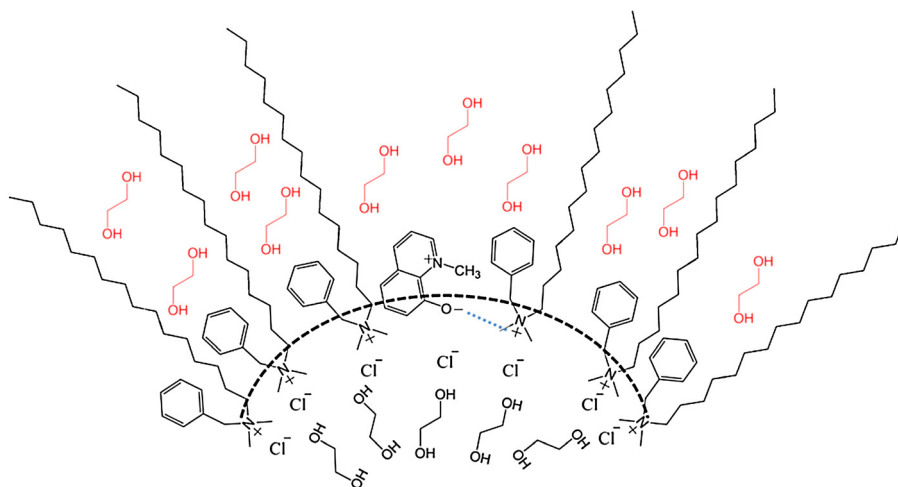


Fig. 7. Schematic representation of the proposed localization of EG molecules in EG/BHDC/*n*-heptane:benzene reverse micelles. In red, the EG molecules localized in oil side of micellar interface are shown. In blue dash line, the interaction between QB molecular probe and nitrogen atom of BHDC surfactant is represented. (For interpretation of the references to colour in this figure legend, the reader is referred to the web version of this article.)

The systems studied using QB were EG/BHDC/*n*-heptane:benzene RMs, at $W_s = 2.5$, and $X_{HP} = 0.00, 0.13$ and 0.21 to investigate the effect that the external solvent blend has on the RMs interfacial properties. We will compare the results obtained in this work with the obtained in previous work, for the system BHDC/*n*-heptane:benzene at $W_s = 0.0$ (i.e., without the addition of EG) [7]. Typical QB absorption spectra varying the BHDC concentration at $W_s = 2.5$ and $X_{HP} = 0.00$ are shown in Fig. 5. Similar spectra are observed in all the RMs investigated (not shown). We have investigated the EG addition up to $W_s = 2.5$ and, in such case, the maximum amount of *n*-heptane that yields transparent RMs solution is $X_{HP} = 0.21$ (Fig. 2 and Table 1).

3.3.1. Analysis of the B1 wavelength

Fig. 6A shows the wavelength values of the absorption maximum of the QB B_1 band (λ_{maxB1}), versus BHDC concentration, in EG/BHDC/*n*-heptane:benzene RMs, at $W_s = 2.5$ and different X_{HP} values. Once RMs are formed, QB is mainly located at the RMs micellar interface, a more polar microenvironment, causing the decrease in λ_{maxB1} values with the increases in the surfactant concentration.

In Fig. 6A it is observed a range in the BHDC concentration where the micropolarity changes dramatically and, the operational critical micellar concentration (cmc) can be obtained for each system and gathered in Table 3. An analysis of the cmc values reveal two conclusions: (i) the EG addition favors the formation of RMs (i.e., at same X_{HP} the cmc values decrease when W_s values increase), and (ii) the *n*-heptane also “benefits” the formation of RMs (i.e., at same W_s , the cmc values decrease when X_{HP} values increase). Similar trends between cmc values with W_s and X_{HP} were obtained previously for water/BHDC RMs, with cmc values of a similar order of magnitude [7,37]. Our data show that, the presence of polar solvent, as EG, favors the RMs formation in comparison with the system without polar solvent. This is probably due because the surfactant molecules will tend to decrease the highest interfacial tension between the polar droplet (EG) and non-polar molecules (as benzene and *n*-heptane), forming the RMs. So this interfacial tension between the polar and non-polar phase is the driving force that favors the RMs formation. In the absence of polar molecules, the interfacial tension, and therefore the driving force, does not exist and the RMs formation is energetically less favorable.

3.3.2. Analysis of absorbances ratio

Fig. 6B shows the Abs B_2 /Abs B_1 ratio values for QB, versus BHDC concentration, in EG/BHDC/*n*-heptane:benzene RMs at $W_s = 2.5$ and

$X_{HP} = 0.00, 0.13$ and 0.21 . In all the systems, it is observed that the Abs B_2 /Abs B_1 values decrease until a BHDC concentration about the value of the cmc, and then begins to increase for higher concentrations of surfactant.

In previous work, we carried out a similar analysis for the Abs B_2 /Abs B_1 values of QB in water/BHDC/*n*-heptane:benzene RMs [7]. A similar trend was obtained: for systems with $X_{HP} = 0.00$ and $X_{HP} = 0.13$, above the value of the cmc, the Abs B_2 /Abs B_1 values increases, independently of polar solvents encapsulated (water or EG). We attributed this trend to an electrostatic interaction (water or EG). We attributed this trend to an electrostatic interaction between the negative charge of QB (the phenolate oxygen) and the positive charge of the BHDC surfactant (cationic head-group), which alters the QB intramolecular charge transfer band, diminishing the molar extinction coefficient of the B_1 band [7]. Thus, a similar interpretation can be invoked for EG/BHDC/*n*-heptane:benzene RMs at $X_{HP} = 0.00$ and 0.13 : in both cases, QB-BHDC interaction is stronger than QB-EG interaction, and above the value of cmc, the absorbance ratio value increases. This can be due to EG molecules penetrate into the non-polar region of the interface [10], as it is shown in Fig. 7, among BHDC tails, where QB molecular probe is not located (QB reside mainly in polar region interface).

On the other hand, if we compare the aqueous and non-aqueous systems for $X_{HP} = 0.21$, can be observed very different behavior. For the system of water/BHDC/*n*-heptane:benzene at $X_{HP} = 0.21$ (inset in Fig. 6B), we observed that QB monitors the water molecules, and the changes in the absorbances ratio values are the expected for a hydrogen bond donor environment [7]. Thus, above the cmc values, the Abs B_2 /Abs B_1 ratio reached a plateau. In contrast, for EG/BHDC/*n*-heptane:benzene at $X_{HP} = 0.21$ we observed that, above the cmc value, the absorbance ratio values increase and, in this case, we could infer that QB does not monitor EG molecules at the interface [7]. As was mentioned above, this can be due to that EG penetrates mostly into the oil side of interface (Fig. 7) allowing the electrostatic interaction between QB and BHDC, with the consequent increases of the absorbance ratio values above the cmc value.

Finally, since EG resides in the oil side of the RM interface, it increases its fluidity, favors the inter-micellar attractions, decreases the capacity of solubilization of polar solvent and increases the size aggregates, in comparison to water/BHDC RMs. In this sense, the “sticky effect” on RMs previously attributed to *n*-heptane solvent [7,16,17], is increased even more by encapsulation of EG molecules.

4. Conclusions

We have presented the first studies performed on non-aqueous cationic RMs formed by EG/BHDC dispersed in *n*-heptane:benzene mixture without the presence of a co-surfactant. We observed that the EG solubilization capacity depends on the external phase composition, and decreases as the *n*-heptane content increases.

Using DLS technique, we demonstrated the presence of RMs, and observed that for the same [EG]/[BHDC] ratio, the micellar size increases when *n*-heptane content increases. We attributed this effect because of *n*-heptane favors the droplet-droplet attractions. We observed that the solubilization capacity and the droplet sizes of the aggregates are significantly different to the one observed for water/BHDC RMs. Thus, we propose that EG changes the interface fluidity, and favors the increment of the inter-micellar attractions, compared to water/BHDC RMs.

Using QB as molecular probe, we determined the critical micellar concentration for EG/BHDC RMs, and observed that the formation of RMs are favored when *n*-heptane content increases. In addition, we demonstrated that EG molecules penetrates into micellar interface, and are mainly located in the oil side of the interface. Consequently, EG change the interface composition, and has a “sticky effect”, enhancing a similar effect exerted by *n*-heptane when is added to benzene. Thus, we hope that the results can be employed in using these RMs as nanoreactors, for example in nanoparticles synthesis, controlling the inter-micellar interactions and thus the sizes and morphologies of the nanoparticles, venue that we are currently investigating.

Acknowledgements

Financial support from the Consejo Nacional de Investigaciones Científicas y Técnicas (CONICET, PIP CONICET 112-201101-00204, Universidad Nacional de Río Cuarto, Agencia Nacional de Promoción Científica y Técnica (PICT 2012-0232), (PICT 2016-2151), and Ministerio de Ciencia y Tecnología, gobierno de la provincia de Córdoba (PID-2012) is gratefully acknowledged. N.M.C., J.J.S. and R.D.F. hold a research position at CONICET. F.M.A. thanks CONICET for a research fellowship.

References

- [1] T.P. Hoar, J.H. Schulman, Transparent water-in-oil dispersions: the oleopathic hydro-micelle, *Nature* 152 (1943) 102–103.
- [2] P. Zheng, Y. Ma, D. Fan, X. Peng, T. Yin, J. Zhao, W. Shen, Solvent dependent interactions between droplets in water-in-oil microemulsions, *Soft Matter* 10 (2014) 7977–7984.
- [3] A. Ganguly, B.K. Paul, S. Ghosh, N. Guchhait, Probing the location of methanol in methanol/AOT/*n*-heptane system: true microemulsion or bi-continuous medium? *RSC Adv.* 4 (2014) 41122–41128.
- [4] A.K. Ganguly, A. Ganguly, S. Vaidya, Microemulsion-based synthesis of nanocrystalline materials, *Chem. Soc. Rev.* 39 (2010) 474–485.
- [5] M.E. Parent, J. Yang, Y. Jeon, M.F. Toney, Z.-L. Zhou, D. Henze, Influence of surfactant structure on reverse micelle size and charge for nonpolar electrophoretic inks, *Langmuir* 27 (2011) 11845–11851.
- [6] V. Stepankova, S. Bidmanova, T. Koudelakova, Z. Prokop, R. Chaloupkova, J. Damborsky, Strategies for stabilization and activation of biocatalysts in organic solvents, *ACS Catal.* 3 (2013) 2823–2836.
- [7] F.M. Agazzi, R.D. Falcone, J.J. Silber, N.M. Correa, Solvent blends can control cationic reversed micellar interdroplet interactions: the effect of *n*-heptane:benzene mixture on BHDC interfacial properties: droplet sizes and micropolarity, *J. Phys. Chem. B* 115 (2011) 12076–12084.
- [8] N.M. Correa, J.J. Silber, R.E. Riter, N.E. Levinger, Nonaqueous polar solvents in reverse micelle systems, *Chem. Rev.* 112 (2012) 4569–4602.
- [9] N.M. Correa, M.A. Biasutti, J.J. Silber, Micropolarity of reverse micelles of AOT in *n*-hexane, *J. Colloid Interface Sci.* 172 (1995) 71–76.
- [10] A.M. Durantini, R.D. Falcone, J.J. Silber, N.M. Correa, Effect of constrained environment on the interaction between the surfactant and different polar solvents encapsulated within AOT reverse micelles, *ChemPhysChem* 10 (2009) 2034–2040.
- [11] A. Salabat, J. Eastoe, K.J. Mutch, R.F. Tabor, Tuning aggregation of microemulsion droplets and silica nanoparticles using solvent mixtures, *J. Colloid Interface Sci.* 318 (2008) 244–251.
- [12] V.R. Vasquez, B.C. Williams, O.A. Graeve, Stability and comparative analysis of AOT/water/isooctane reverse micelle system using dynamic light scattering and molecular dynamics, *J. Phys. Chem. B* 115 (2011) 2979–2987.
- [13] E.M. Corbeil, N.E. Levinger, Dynamics of polar solvation in quaternary microemulsions, *Langmuir* 19 (2003) 7264–7270.
- [14] A.M. Dokter, S. Woutersen, H.J. Bakker, Ultrafast dynamics of water in cationic micelles, *J. Chem. Phys.* 126 (2007) 124507.
- [15] L. Klicocova, P. Sebej, P. Stacko, S.K. Filippov, A. Bogomolova, M. Padilla, P. Klan, CTAB/water/chloroform reverse micelles: a closed or open association model? *Langmuir* 28 (2012) 15185–15192.
- [16] F.M. Agazzi, J. Rodriguez, R.D. Falcone, J.J. Silber, N.M. Correa, PRODAN dual emission feature to monitor BHDC interfacial properties changes with the external organic solvent composition, *Langmuir* 29 (2013) 3556–3566.
- [17] F.M. Agazzi, N.M. Correa, J. Rodriguez, Molecular dynamics simulation of water/BHDC cationic reverse micelles: structural characterization, dynamical properties and the influence of the solvent on the intermicellar interactions, *Langmuir* 30 (2014) 9643–9653.
- [18] R. McNeil, J.K. Thomas, Benzylhexadecyldimethylammonium chloride in microemulsions and micelles, *J. Colloid Interface Sci.* 83 (1981) 57–65.
- [19] A. Jada, J. Lang, R. Zana, R. Makhlofi, E. Hirsch, S.J. Candau, Ternary water in oil microemulsions made of cationic surfactants water, and aromatic solvents. 2. Droplet sizes and interactions and exchange of material between droplets, *J. Phys. Chem.* 94 (1990) 387–395.
- [20] R.D. Falcone, N.M. Correa, J.J. Silber, On the formation of new reverse micelles: a comparative study of benzene/surfactants/ionic liquids systems using UV–vis absorption spectroscopy and dynamic light scattering, *Langmuir* 5 (2009) 10426–10429.
- [21] N.M. Correa, M.A. Biasutti, J.J. Silber, Micropolarity of reverse micelles: comparison between anionic, cationic and neutral reverse micelles, *J. Colloid Interface Sci.* 184 (1996) 570–578.
- [22] J.J. Florez Tabares, N.M. Correa, J.J. Silber, L.E. Sereno, P.G. Molina, Droplet droplet interactions investigated using a combination of electrochemical and dynamic light scattering techniques. The case of water/BHDC/benzene:*n*-heptane system, *Soft Matter* 11 (2015) 2952–2962.
- [23] H. Yue, Y. Zhao, X. Ma, J. Gong, Ethylene glycol: properties, synthesis, and applications, *Chem. Soc. Rev.* 41 (2012) 4218–4244.
- [24] L.P. Novaki, N.M. Correa, J.J. Silber, O.A. El Seoud, FT-IR and ¹HNMR studies of the solubilization of pure and aqueous 1,2-ethanediol in the reverse aggregates of Aerosol-OT, *Langmuir* 16 (2000) 5573–5578.
- [25] S. Ray, S.P. Moulik, Dynamics and thermodynamics of aerosol OT-aided nonaqueous microemulsions, *Langmuir* 10 (1994) 2511–2515.
- [26] S.K. Mehta, Kawaljit, Phase diagram and physical properties of a waterless sodium bis(2-ethylhexylsulfosuccinate)-ethylbenzene-ethyleneglycol microemulsion: an insight into percolation, *Phys. Rev. E* 65 (2002) 021502.
- [27] S.K. Mehta, Kawaljit, K. Bala, Phase behavior, structural effects, and volumetric and transport properties in nonaqueous microemulsions, *Phys. Rev. E* 59 (1999) 4317–4325.
- [28] Y. Sun, Y. Xia, Shape-controlled synthesis of gold and silver nanoparticles, *Science* 298 (2002) 2176–2179.
- [29] C. Li, K.L. Shuford, M. Chen, E.J. Lee, S.O. Cho, A facile polyol route to uniform gold octahedra with tailorable size and their optical properties, *ACS Nano* 2 (2008) 1760–1769.
- [30] S.E. Skrabalak, B.J. Wiley, M. Kim, E.V. Formo, Y. Xia, On the polyol synthesis of silver nanostructures: glycolaldehyde as a reducing agent, *Nano Lett.* 8 (2008) 2077–2081.
- [31] P. Setua, R. Pramanik, S. Sarkar, C. Ghatak, S.K. Das, N. Sarkar, Synthesis of silver nanoparticle inside the nonaqueous ethylene glycol reverse micelle and a comparative study to show the effect of the nanoparticle on the reverse micellar aggregates through solvation dynamics and rotational relaxation measurements, *J. Phys. Chem. B* 114 (2010) 7557–7564.
- [32] M. Ueda, Z.A. Schelly, Reverse micelles of Aerosol-OT in benzene. 4. Investigation of the micropolarity using 1-methyl-8-oxyquinolinium betaine as a probe, *Langmuir* 5 (1989) 1005–1008.
- [33] H. Iloukhani, M.R. Sameti, J.B. Parsa, Excess molar volumes and dynamic viscosities for binary mixtures of toluene + *n*-alkanes (C5–C10) at T = 298.15 K. Comparison with Prigogine–Flory–Patterson theory, *Chem. Thermodyn.* 38 (2006) 975–982.
- [34] V.R. Vasquez, B.C. Williams, O.A. Graeve, Stability and comparative analysis of AOT/water/isooctane reverse micelle system using dynamic light scattering and molecular dynamics, *J. Phys. Chem. B* 115 (2011) 2979–2987.
- [35] P.A. Hassan, S. Rana, G. Verma, Making sense of Brownian motion: colloid characterization by dynamic light scattering, *Langmuir* 31 (2015) 3–12.
- [36] R.E. Riter, J.R. Kimmel, E.P. Undiks, N.E. Levinger, Novel reverse micelles partitioning nonaqueous polar solvents in a hydrocarbon continuous phase, *J. Phys. Chem. B* 101 (1997) 8292–8297.
- [37] R.D. Falcone, N.M. Correa, M.A. Biasutti, J.J. Silber, Properties of AOT aqueous and nonaqueous microemulsions sensed by optical molecular probes, *Langmuir* 16 (2000) 3070–3076.